NANO LETTERS

2007
Vol. 7, No. 8
2491−2498

Nanoscale Ion Mediated Networks in Bone: Osteopontin Can Repeatedly Dissipate Large Amounts of Energy

Georg E. Fantner,*,† Jonathan Adams,† Patricia Turner,† Philipp J. Thurner,† Larry W. Fisher,‡ and Paul K. Hansma†

University of California Santa Barbara, Department of Physics, Santa Barbara, California 93106, and Craniofacial and Skeletal Diseases Branch, NIDCR, NIH, DHHS, Bethesda, Maryland 20892

Received May 30, 2007; Revised Manuscript Received July 9, 2007

ABSTRACT

In the nanocomposite bone, inorganic material is combined with several types of organic molecules, and these complexes have been proposed to increase the bone strength. Here we report on a mechanism of how one of these components, human osteopontin, forms large mechanical networks that can repeatedly dissipate energy through work against entropy by breaking sacrificial bonds and stretching hidden length. The behavior of these in vitro networks is similar to that of organic components in bone, acting as an adhesive layer in between mineralized fibrils.

The remarkable mechanical properties of bone, difficulties in diagnosing fracture risk in patients, as well as the severe pathological consequences of bone degeneration have, in addition to detailed investigations into the macroscopic fractures,[1−6] led to increased interest in the nanoscale origin of its toughness. Bone is a nanocomposite consisting of mineralized type I collagen fibrils and a nonfibrillar organic matrix.[7] There is increasing evidence that mechanisms at the nanometer scale play an important role in the dissipation of mechanical energy when bone is deformed. X-ray diffraction has revealed that tensile strain in bone is divided into tensile stretching of mineralized collagen fibrils and shear deformation of the interfibrillar matrix.[8,9] This suggests that the hierarchical design of bone at the nanometer scale leads to a hierarchical and coupled deformation mechanism between the collagen fibrils, the mineral particles, and the extrafibrillar matrix.[10] It has been further suggested that disruption of weak bonds between polyelectrolyte molecules in the extrafibrillar matrix of bone (perhaps mediated by polyvalent ions) may be a significant energy dissipation mechanism.[9,11] Macroscopic test of the influence of ion concentration on bone strength have shown a reversible influence of the presence of Ca^{2+} ions on the mechanical behavior of mineralized bone tissue at the macro scale.[12] Quantitative nanoindentation suggests the importance of interparticle friction and intraorganic matrix cohesion for the resistance in compression.[13] In most of these mechanisms, the extrafibrillar organic matrix transfers strain and dissipates energy. In this paper, we investigate how the extrafibrillar matrix achieves this on the molecular level. As a model system of the interfibrillar matrix, we study the mechanical properties of thin layers of one of the most abundant noncollagenous proteins in bone (5−10% of noncollagenous proteins in bone), human osteopontin, which is (among other places) found in bone[14] and arterial plaque buildup.[15,16] We find that human osteopontin can form networks stabilized with sacrificial bonds. These networks can dissipate large amounts of energy through the breaking of sacrificial bonds but mainly the stretching of hidden length without the need for folded domains within the protein.

Recently, we reported evidence for the existence of a molecular adhesive with sacrificial bonds and hidden length within the nanocomposite bone holding the mineralized collagen fibrils together.[11] This adhesive is visible in high-magnification images of bone (see Figure 1A) and detectable in molecular pulling experiments with the atomic force microscope (AFM), where forces were measured over a range of several micrometers.[11] Which components of the organic matrix of bone contribute to this adhesion has, however, not been determined.

In addition to bone, it has been shown for a number of natural materials that an organic matrix greatly improves the material strength.[17−21] Explanations for this improvement range from crack deflection[20] and crack arrest at boundaries[22] to shock absorption and self-healing repair after energy dissipation in the form of sacrificial bonds and hidden length.[11,18,23] This energy dissipation comes, in large part, from work against the entropic elasticity of molecules with sacrificial bonds and hidden lengths.[18,24,25] Unlike titin and

* Corresponding author. E-mail: fantner@physics.ucsb.edu.
† University of California Santa Barbara, Department of Physics.
‡ Craniofacial and Skeletal Diseases Branch, NIDCR, NIH, DHHS.

10.1021/nl0712769 CCC: $37.00
Published on Web 07/24/2007

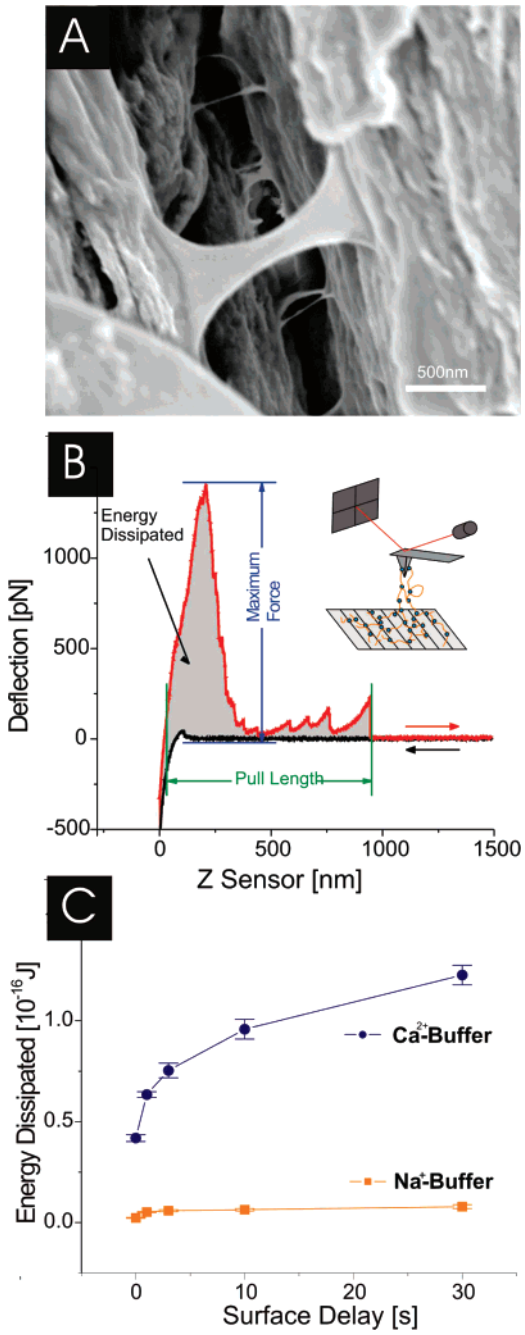

Figure 1. AFM multiple molecule force spectroscopy can be used to investigate adhesive properties of purified molecules as well as mixtures of molecules from nature as previously reported for bone.[11] (A) SEM micrograph showing remnants of an organic adhesive spanning the gap between a microcrack in bone. (B) Example force spectroscopy (pulling) curve on a thin layer of osteopontin, defining the three measured parameters. The inset shows an artist's conception of a network of molecules without tertiary structure being pulled by the AFM tip. (C) The time dependence of the adhesion (energy dissipation) within a thin layer of recombinant osteopontin (OPN) is influenced by the presence of Ca^{2+}, a result similar to the behavior of the adhesive between mineralized collagen fibrils in bone.[11]

fibronectin,[26−28] however, other proteins like osteopontin lack the folded modular domains commonly associated with sacrificial bonds and hidden lengths.

Force spectroscopy of proteins with folded tertiary structure has given a wealth of information about the molecular interactions that stabilize the structure not only when the proteins are in buffer solution[29] but also when they are in membranes covered with buffer solution.[30] Engineered recombinant constructs with repeated modules of precisely known amino acid sequence have revealed that even changes of single amino acids can have reproducibly measurable effects on single-molecule force spectra.[31] Many of these proteins such as titin and fibronectin are known to play a mechanical role in tissues.[32,33]

In addition to yielding information about single protein molecules with precisely folded tertiary structure, pulling experiments with the atomic force microscope can yield useful information about the mechanical behavior of ensembles of multiple recombinant protein molecules with no tertiary structure.[24,34,35] Figure 1B shows three parameters that can be measured even in the absence of pronounced tertiary structure: the maximum adhesion force (maximum peak height), the maximum pulling distance (pulling length at which all connections between cantilever and surface are broken), and the total energy dissipation (area under the curve).

In addition to its hypothesized role in the regulation of mineralization of collagen,[36] osteopontin, an abundant noncollagenous component of the organic matrix of bone, was proposed to act as a mediator of cell−matrix and matrix−matrix/mineral as well as mineral−mineral adhesion in mineralized tissue interfaces such as cement lines in bone and boundaries to titanium implants.[37] Here we report that layers of recombinant osteopontin (OPN) exhibit energy dissipation over the range of micrometers through sacrificial bonds and hidden length despite having no folded tertiary structure in solution and a macromonomer length of only 100 nm.[28]

In our experiments, we used recombinant human OPN that was dissolved in purified water at a concentration of 2 μg/ul. Then 4 μl of solution was deposited on freshly cleaved mica, then dried and rehydrated. Immersed in our test buffers, we used Biolevers (model OBL-105, Olympus Corp., Tokyo, Japan) with a nominal spring constant $k = 0.02$ N/m and a MultiMode AFM system with PicoForce (Veeco Inc., Santa Barbara, CA). For the pulling experiments of Figure 1C, the cantilever was pushed on the mica with 500 pN for 0, 1, 3, 10, and 30 s and retracted 1.5 μm at a rate of 0.317 Hz, i.e., 0.95 μm/s, at two spots. More than 400 pulls per test buffer were recorded. The energy dissipation of these pulls is plotted as a function of the surface retention time in Figure 1C for experiments conducted in Na buffer (150 mM NaCl, 10 mM Hepes, pH 7.4) and Ca buffer (40 mM $CaCl_2$, 110 mM NaCl, 10 mM Hepes, pH 7.4), respectively. It is remarkable that, in these pulls, relatively large amounts of energy are dissipated and that the energy dissipation increases with the presence of Ca^{2+} ions in a similar manner to the adhesive in bone.[11,23] Figure 1C shows the total energy dissipation as a function of surface retention time of pulls on recombinant osteopontin (OPN) with posttranslational modifications as described in the Methods section. One hundred pulls have been performed for each surface retention time; error bars represent the standard deviation.

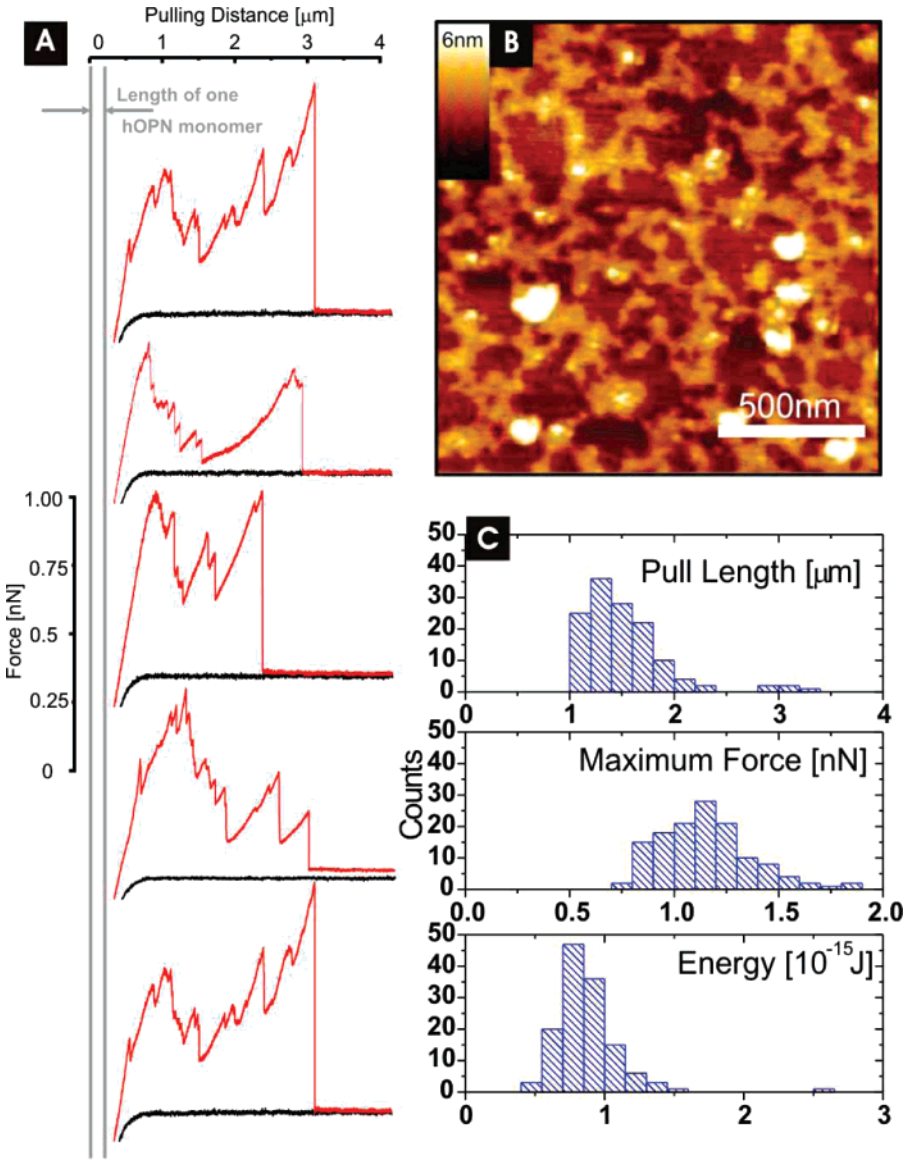

Figure 2. OPN macromonomers can form long continuous networks. (A) Example force pulls on a dense layer of recombinant OPN. The length the cantilever can be retracted before molecular connection breaks is many times the length of one OPN macromonomer. The shape of the pulling curves suggests the entanglement of the molecules in a network. (B) AFM image of a thin layer of OPN deposited on mica. The OPN molecules form a continuous network with stretches distances on the order of μm. (C) Distribution of the pulling length, maximum force, and energy dissipation of more than hundred pulls. The average pulling length is over 1 μm, which corresponds to more than 10 OPN macromonomers if they were aligned end-to-end in one chain. The average maximum pulling force (for this sample coverage) is on the order of 1 nN, which, when the molecules are connected in a network, puts the sacrificial bond strength on the order of 100 pN.

The actual shape of the pulling curve indicates the mechanism by which OPN dissipates this large amount of energy. Figure 2A shows a series of representative pulling curves on a dense layer of OPN. The pulling curves extend over several micrometers, which is remarkable given that the estimated contour length of an extended osteopontin macromonomer is approximately 100 nm (assuming an average length of 3.5 Å per amino acid and 298 amino acids). This suggests that OPN can form long aggregate networks. In the curves, peaks are followed by both higher and lower peaks, suggesting that the OPN molecules being pulled on are arranged in a network between the tip and the surface.[24] AFM images of a diluted solution of osteopontin, deposited on a mica surface, shows such a network of the OPN molecules, Figure 2B (in order to better visualize the network, the osteopontin concentration was reduced by a factor of 10 compared to that of the pulling experiments). Although OPN is believed to be extended and fully flexible in solution, it is possible that OPN adopts a specific structure in relation to its binding partner.[28] Figure 2C shows the statistical distribution of the pulling length to rupture, the maximum force, and the energy dissipation over several hundred pulls. It is important to note that, on samples with different surface coverage, the pulling length and therefore the dissipated energy can differ drastically. More osteopontin will result in longer range adhesion and more energy dissipation.

The results shown in Figure 1C indicated that the degree with which the network resisted the applied force of the cantilever increased dramatically with the presence of Ca^{2+}

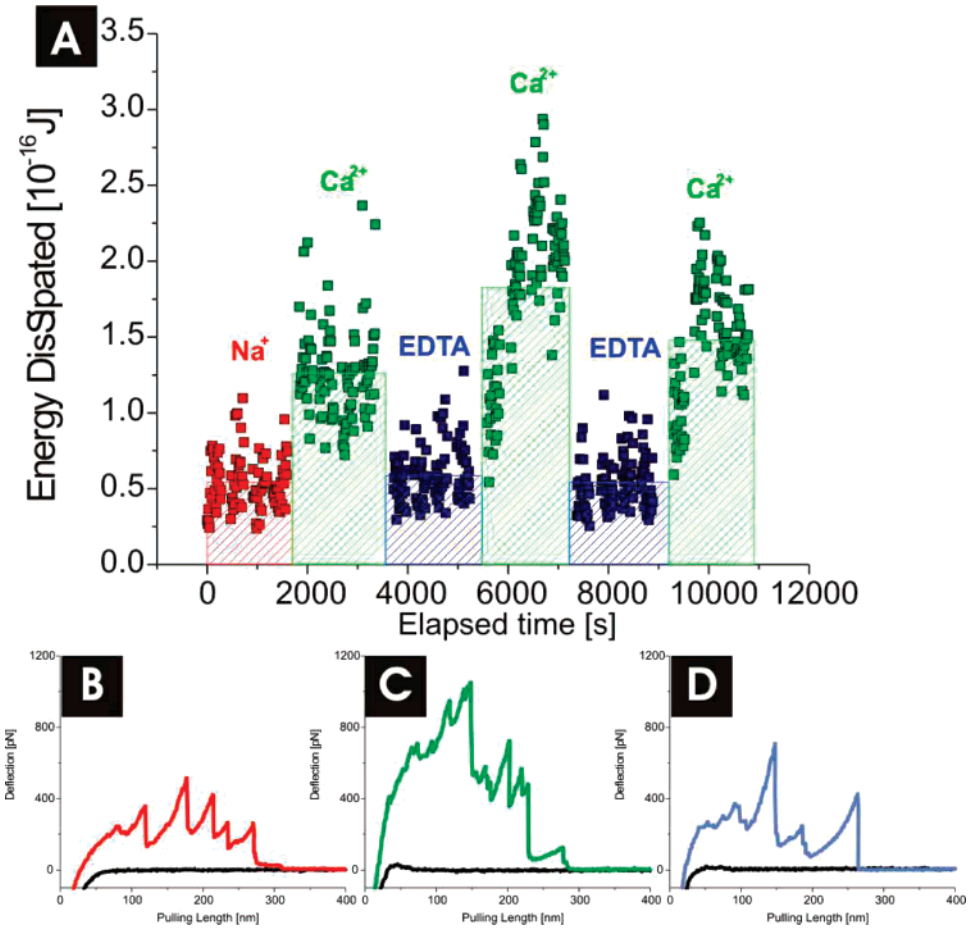

Figure 3. Switchable network strength in a dilute OPN layer and dependence on presence of divalent cations. (A) Energy dissipation of force spectroscopy pulls for a sample treated consecutively with Na^+, Ca^{2+}, EDTA, Ca^{2+}, EDTA, and Ca^{2+}. Each square represents one pull; the shaded bars represent the averages of the pulls in that sequence. The energy dissipation increases significantly with the addition of Ca^{2+} ions. After chelation of the Ca^{2+} ions with 250 mM excess of EDTA, the energy dissipation comes back to the original level. This "switching off" and "switching on" of the adhesion can be repeated multiple times. (B,C,D) Representative curves of the pulls in Na^+ buffer, Ca^{2+} buffer, and EDTA, respectively.

ions. We therefore expect the Ca^{2+} ions to enhance the strength of the formed network. Figure 3 shows a series of pulling curves where the strength of a particular area of one network was probed as a function of ions in the surrounding solution. Pulling experiments were started on a network in a buffer (ph 7.4) containing only Na^+ as cations to establish a baseline (red section in Figure 3A), after which 200 μL of buffer (ph 7.4) containing Na^+ and Ca^{2+} were added. Pulling rate and threshold force were the same as for the previously described experiments. One hundred pulls were recorded for each buffer type, each time after 25 pulls, a new 200 μL of the current buffer was flushed through the AFM fluid cell to make sure that changes are due to a change in ions and not just due to the act of exchanging fluid (e.g., removal of OPN due to fluid exchange). The average energy dissipation per pull doubled over a relatively short time scale (10−100 s, green section in Figure 3A). This change in energy dissipation does not directly reverse when flushing with Na buffer (data not shown), indicating that the Ca^{2+} ions are still contained in the network. The Ca^{2+} ions are not, however, irretrievably bound within the network. After chelating the Ca^{2+} ions with excess of ethylenediaminetetraacetic acid (EDTA) (250 mM, pH 8), the energy dissipation drops down to the initial level within a short period of time. This process of increasing and decreasing the energy dissipation by adding and removing Ca^{2+} ions is repeatable, as shown in this dataset for three consecutive fluid exchanges. Parts B, C, and D of Figure 3 show representative curves for the pulls in Na^+, Ca^{2+}, and EDTA, respectively. It is important to note that the absolute values of the energy dissipation (as well as the pulling length) in these experiments depends strongly on the thickness and distribution uniformity of the osteopontin layer. To minimize the influence of the distribution, we performed the pulling experiments in a grid of 5 × 5 with a spacing of 1 um. This grid was cycled through four times per buffer change so that multiple pulling curves were recorded for each spot but separated in time. Nevertheless, the absolute values of the energy dissipation between different experiments could vary by almost an order of magnitude. To compare several experiments we normalized the energy dissipation to the average level of the pulls in sodium and saw that the relative change of energy dissipation when Ca^{2+} ions were added was present in all experiments.

The formation of the networks and the shape of the pulling curves suggest a calcium-mediated binding between the OPN

molecules. This is consistent with light-scattering measurements that showed a calcium-enhanced polymerization reaction for another phosphorylated protein, bone acidic glycoprotein-75.[38] The average maximum pulling force is 1.1 nN in our experiments on OPN (Figure 2C). We know that the force is distributed over several molecules.[24] In the example curves of Figure 2A, we observe on the order of 10 major peaks per pull. The minimum individual bond strength (if all force peaks represent parallel molecules, which we know is not the case) would be on the order of 100 pN. If all molecules were chained together in series, the individual bond strength would need to be 1.1 nN, but this extreme case is also not consistent with the multiple peaks in the pulling curves. The strength of the calcium-mediated bond will therefore be somewhere in between the two values, 100 pN and 1.1 nN, which corresponds well with the previously recorded average force for sacrificial bonds in other systems.[25] Typically, those bonds would have a bond-breaking energy on the order of an electronvolt (1.6×10^{-19} J), however, this is several orders of magnitude smaller than the dissipated energy reported in Figures 2 and 3. Indeed, the energy of 10^{-15} J given in Figure 2 corresponds to the binding energy of 1700 covalent C−C bonds. The apparent discrepancy of these numbers can be explained by the probable shape of a random network. Figure 4 shows a schematic of how the osteopontin molecules could form random connections between mineralized fibrils. If the osteopontin molecules are arranged in a quasirandom network (which we propose based on the many charged side groups distributed along the molecule that could interact with Ca^{2+} ions), a force applied to the whole network will not be distributed equally over all molecules. Some molecules (dotted molecules in Figure 4) will be (partially) shielded from that force by sacrificial bonds (circles in Figure 4). When stretching a chain of molecules, the largest part of the energy goes into work against entropy to linearize the chain;[24,25] we therefore treat the molecule for this discussion as an entropic spring. When the molecule is stretched out and the force reaches the level required to break the sacrificial bond, molecules that were previously shielded from the force will now also contribute to the effective length of the connection, which increases the entropy relevant for the force extension behavior. To linearize the connections again, more work against the entropy has to be applied. This process continues until the last connection between the surfaces breaks. The gain in energy dissipation by adding the sacrificial bonds that shield the hidden length is depicted in the force curve of Figure 4E as the dotted area. The energy dissipation from the breaking of the sacrificial bonds is by comparison insignificant. The sacrificial bonds however do not have to occur only in between the molecules but could also be formed between the molecules and the surfaces. In our experiment, the Ca^{2+} can also enhance the adhesion of the highly charged osteopontin to the OH groups of the mica. This interaction could be compared to the binding of the glue molecules to the OH groups of the hydroxyapatite particles of mineralized fibrils.

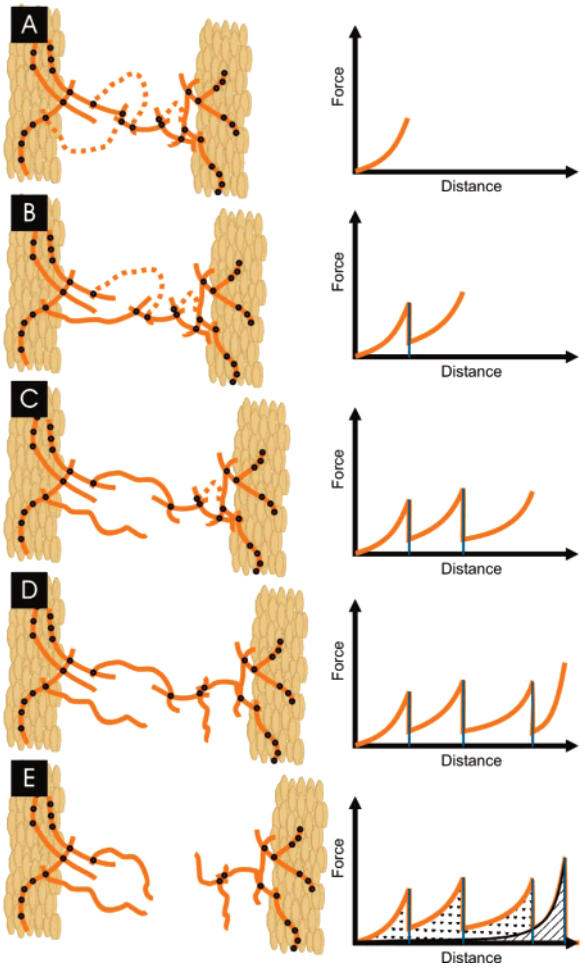

Figure 4. Artist rendering of the proposed model for the increased energy dissipation. (A) In the random network, not all connections are equally long, hence when stretched, not all molecules feel the force immediately (dotted molecules) as they are shielded by the sacrificial bonds (circles) that form the network. The approximate effective length that connects the two sides is the shortest path along the solid line molecules, which results in a rather steep initial increase in the force distance curve. (B) At the force when one of the sacrificial bonds breaks, a small amount of energy goes into this breaking (ca. 1 eV). Then a molecule part previously shielded from the force now contributes to the unstretched length and more work has to be applied against the entropy of the additional length. This process continues (B−D) until all the sacrificial bonds that shield hidden length (relevant for that particular connection) are broken and the two surfaces are separated (E). The energy dissipation that is gained by the revealing of hidden length is the dotted area in the force curve of panel (E).

It has long since been an area of debate of where failure occurs if bone is stressed beyond the elastic limit and where the energy dissipation takes place. Gupta et al. propose viscous flow of the matrix past the fibrils, where the energy dissipation occurs through friction on the high aspect ratio and high surface area of the fibrils[39] as well as some additional internal decohesion between mineral particles and collagen. Gupta et al. found an activation energy of 1.1 eV associated with the basic step involved in the plastic deformation of bone at the molecular level.[9] They note that this is much higher than the energy of hydrogen bonds, but it is lower than the energy required for breaking covalent bonds inside the collagen fibrils. On the basis of the

magnitude of these quantities, they speculated that disruption of electrostatic bonds between polyelectrolyte molecules in the extrafibrillar matrix of bone, perhaps mediated by polyvalent ions such as calcium, may be the rate-limiting elementary step in bone plasticity.[9] This is consistent with our hypothesis[11] for a mechanism based on sacrificial bonds and hidden lengths[7,11,23,40] because it supports the idea that bonds of intermediate strength, which is just what is wanted for sacrificial bonds, are involved in the plastic deformation of bone at the molecular level. Tai, Ulm, and Ortiz found nanoindentation evidence that suggests that cohesion values in compression are attributable to the organic itself, rather than interfacial mineral−organic bonding.[13] Our findings in this paper are consistent with these hypotheses, offering a molecular mechanism of how the molecules of the nonfibrillar organic matrix dissipates the large amount of energy required for the toughness of bone within the matrix as well as on the interface. Thurner et al. as well as Kindt et al. conclude from scanning electron microscopy (SEM) and AFM studies that bone fails within the interfibrillar interface.[41,42] In their article, Kindt et al. attributed the reduced mechanical properties of bone treated with sodium fluoride solution to mineral−collagen debonding, proposing that the fluoride decreased the affinity of the mineral particles to the organic matrix.

The network formation is however not unique to OPN. Experiments on two other proteins from the same small integrin binding ligand, N-linked glycoprotein (SIBLING) family, bone sialoprotein (BSP) (also shown by NMR to be unstructured in solution[28]), and dentin matrix protein-1 (DMP1) (structure unknown), show a similar network-forming behavior which increases in the presence of calcium ions (data not shown). The fact that all these proteins have large amounts of a number of different acidic post-translational modifications, including sialic acid-containing carbohydrate groups (10 sialic acid containing side groups in OPN), phosphorylated-serine (34 residues, 11.4% of all residues)/threonine (2 residues, 0.7%), and/or sulfated tyrosine (4 residues, 1.3%) as well as the negatively charged amino acids aspartate (48 residues, 16.1%) and glutamate (27 residues, 9.1%), lets us speculate that these strongly anionic groups, together with the Ca^{2+} ions give the strength to the networks. It is not exactly known how many of the residues that theoretically can be phosphorylated are actually phosphorylated in osteopontin from bone or other tissues. OPN from milk contains significantly more phosphorylations than OPN in mineral tissues.[43] The OPN we used was mid-peak in an anion exchange column and so represented neither the most nor least phosphorylated/sialated OPN made by human bone marrow stromal cells. Even without any post-translational modifications, osteopontin contains large amounts of glutamic acid that could bind Ca^{2+}. Further investigations into the influence of the content of these acidic post-translational modifications, along with charge density on the network strength, could clarify this.

Osteopontin is known to be a multifunctional glycoprotein, playing an important role in many biological systems. In addition to the intensively studied regulatory functions of osteopontin,[36,38] there is evidence that osteopontin also acts as a structural component in vivo. McKee and Nanci have suggested that osteopontin acts as an adhesive in cell−matrix and matrix−matrix/mineral interactions.[37] Giachelli et al. have proposed a potential role of osteopontin in cardiovascular disease,[44] plaque buildup and pathogenesis of cardiovascular lesions and repair of mitochondrial wounds.[15] OPN was also previously identified by Qiu et al. to influence the formation of calcium oxalate monohydrate (COM) crystals, which are the major inorganic component in human kidney stones,[45] and Sheng et al. probed the adhesion of AFM cantilevers functionalized with COO^- end groups to such COM crystals.[46] In these experiments, the adhesion force of the tip to one particular COM crystal face (100) increased by a factor of about 2.5 in the presence of Ca^{2+} ions. In bone, two major noncollagenous proteins, bone sialoprotein and osteopontin, have been shown to distribute and accumulate in cement lines and in the spaces along the mineralized collagen fibrils,[47] where they are suggested to have an adhesive function. Recent studies on OPN-deficient mouse bones showed that OPN-deficient bones displayed increased elastic modulus but decreased strength and ductility.[48]

We hypothesize that the type of Ca^{2+} mediated network formation that we report here may be a mechanism for the previously reported adhesive functions of osteopontin[15,36−38,44−47] (in addition to the known RGD receptor-based cell adhesion[44]). Our studies do not, however, imply that pure osteopontin networks play a unique mechanical role in bone or any other biological structures. On the contrary, we expect that Ca^{2+}-mediated network formation and mechanical energy dissipation can play a role with many proteins, especially ones with strongly anionic groups such as the SIBLING proteins studied in this paper. A previous calculation[11] estimated that already 2% of the noncollagenous organic matrix (such as osteopontin) in the interface between the mineralized fibrils in bone would be sufficient to account for the tensile strength of bone. Although OPN is not an abundant protein in bone compared to type I collagen (approximately 0.5% of total protein), it could be sufficient to account for significant amounts of the tensile strength in specific locations. For example, significant energy-dissipating effects may occur at the location of the cement lines (that represent $<10\%$ of bone volume), where the local concentrations of OPN would be much higher than the total bone average. In our experiment, we believe to be pulling on several layers of OPN, making it roughly comparable to the amount of material seen in SEM images. We expect however that nonfibrillar collagen or other noncollagenous proteins such as other glycoproteins, as well as proteoglycans[49] known to be present in bone[50] could also be involved in real adhesive networks in biological structures.

We have shown that the sacrificial bonds and hidden length mechanism is not limited to molecules with globular domains. The effectiveness of relatively short molecules forming networks to dissipate energy suggests a strategy for use in (bio-)nanocomposites. Large amounts of energy that can be dissipated in such networks can be explained by the

additional work against entropy that is required to stretch the hidden length in the network rather than the energy required to actually break the sacrificial bonds. Purified, recombinant osteopontin is an example of a protein forming such a network. This network behaves similarly to the previously reported interfacial glue between mineralized collagen fibrils in bone; we hypothesize therefore that osteopontin, in addition to other similar molecules present in bone such as bone sialoprotein, can act as this interfacial glue through the described network formation. It opens the possibility that small polymer molecules that have side groups, which can form weak, reversible bonds within and between molecules may be useful as interfacial layers of engineered high-performance nanocomposites as well. More detailed knowledge of the mechanism of this network formation and the influence of outside parameters will certainly aid in this effort.

Materials and Methods. Recombinant human OPN was made and purified as previously described.[51] Briefly, an adenovirus-encoding human OPN message was used to infect human bone marrow fibroblasts, cells shown to produce recombinant proteins with good post translational modification such as glycosylation and sulfation. The amino acid sequence of human OPN is: IPVKQADSGS SEEKQLYNKY PDAVATWLNP DPSQKQNLLA PQNAVSSEET NDFKQETLPS KSNESHDHMD DMDDEDDDDH VDSQDSIDSN DSDDVDDTDD SHQSDESHHS DESDELVTDF PTDLPATEVF TPVVPTVDTY DGRGDSVVYG LRSKSKKFRR PDIQYPDATD EDITSHMESE ELNGAYKAIP VAQDLNAPSD WDSRGKDSYE TSQLDDQSAE THSHKQSRLY KRKANDESNE HSDVIDSQEL SKVSREFHSH EFHSHEDMLV VDPKSKEEDK HLKFRISHEL DSASSEVN. Table 1 shows the relative percentages of each amino acid. The mesenchymal cells also have good capability of phosphorylating the proteins. Osteopontin has 36 possible phosphorylation sites (34 Ser, 2 Thr, 4 Tyr; source: Netphos 2.0[52]), which results in 13.4% of the protein to be potentially phosphorylated. The actual number of phosphate and sialic acid groups on the OPN is not known. Acidic O-linked carbohydrate groups were observed by changing of running pattern and metachromatic shift with StainsAll dye (Sigma-Aldrich, St. Louis, MO). Earlier tests had shown that the acidic property of the O-linked carbohydrate groups were due to members of the sialic acid family and are safely assumed to be so for this preparation of OPN. Serum-free media, in which OPN constituted ~50% of the total protein, was diluted 1:1 with water and chromatographed under nondenaturing conditions on anion exchange resin (Toyo-Pearl TSK QAE, Tosoh Bioscience, Tokyo, Japan). Mid-peak OPN fractions were pooled, dialyzed against water, lyophilized, and used as the source of protein for the studies reported here. It is estimated to be >95% pure, as determined by SDS PAGE using both Coomassie Blue and StainsAll stains. No other proteins (Coomassie) or DNA/RNA (StainsAll) are detected on the gels. Similarly purified OPN was previously used for several biochemical studies, for example NMR analysis, where no structured protein peaks (OPN or contaminants) were observed.[28]

Table 1. Relative Amino Acid Composition of Human OPN

residue	number	percentage
A Ala	14	4.7
B Asx	0	0.0
C Cys	0	0.0
D Asp	48	16.1
E Glu	27	9.1
F Phe	7	2.4
G Gly	6	2.0
H His	16	5.4
I Ile	7	2.4
K Lys	19	6.4
L Leu	16	5.4
M Met	4	1.3
N Asn	12	4.0
P Pro	15	5.0
Q Gln	14	4.7
R Arg	9	3.0
S Ser	42	14.1
T Thr	14	4.7
V Val	18	6.0
W Trp	2	0.7
X Unk	0	0.0
Y Tyr	8	2.7
Z Glx	0	0.0
total	298	100.0
	Possibly Phosphorylated[52]	
S Ser	34	11.4
T Thr	2	0.7
Y Tyr	4	1.3

Acknowledgment. This work was supported by the National Science Foundation through the UCSB Materials Research Laboratory under award DMR00-80034, by the National Institutes of Health under award RO1 GM65354, by the NASA University Research, Engineering, and Technology Institute on Bio-inspired Materials under award no. NCC-1-02037, by a research agreement with Veeco no. SB030071. This research was also supported in part (L.W.F.) by the Intramural Research Program of the NIDCR, NIH. G.F. thanks the Austrian Academy of Science for a DOC fellowship. P.J.T. thanks the Swiss National Science Foundation for postdoctoral fellowship PA002-111445.

References

(1) Turner, C. H.; Burr, D. B. *Bone* **1993**, *14*, 595−608.
(2) Ruegsegger, P.; Koller, B.; Muller, R. *Calcif. Tissue Int.* **1996**, *58*, 24−29.
(3) Zioupos, P.; Currey, J. D. *Bone* **1998**, *22*, 57−66.
(4) Keaveny, T. M.; Hayes, W. C. *J. Biomech. Eng.* **1993**, *115*, 534−542.
(5) Silva, M. J.; Keaveny, T. M.; Hayes, W. C. *J Orthop. Res.* **1998**, *16*, 300−308.
(6) Bay, B. K.; Smith, T. S.; Fyhrie, D. P.; Saad, M. *Exp. Mech.* **1999**, *39*, 217−226.
(7) Fantner, G. E.; Rabinovych, O.; Schitter, G.; Thurner, P.; Kindt, J. H.; Finch, M. M.; Weaver, J. C.; Golde, L. S.; Morse, D. E.; Lipman, E. A.; Rangelow, I. W.; Hansma, P. K. *Compos. Sci. Technol.* **2006**, *66*, 1205−1211.
(8) Gupta, H. S.; Wagermaier, W.; Zickler, G. A.; Aroush, D. R. B.; Funari, S. S.; Roschger, P.; Wagner, H. D.; Fratzl, P. *Nano Lett.* **2005**, *5*, 2108−2111.
(9) Gupta, H. S.; Fratzl, P.; Kerschnitzki, M.; Benecke, G.; Wagermaier, W.; Kirchner, H. O. *J. R. Soc. London, Interface* **2007**, *4*, 277−282.

(10) Gupta, H. S.; Seto, J.; Wagermaier, W.; Zaslansky, P.; Boesecke, P.; Fratzl, P. *Proc. Natl. Acad. Sci. U.S.A.* **2006**, *103*, 17741−17746.
(11) Fantner, G. E.; Hassenkam, T.; Kindt, J. H.; Weaver, J. C.; Birkedal, H.; Pechenik, L.; Cutroni, J. A.; Cidade, G. A. G.; Stucky, G. D.; Morse, D. E.; Hansma, P. K. *Nat. Mater.* **2005**, *4*, 612−616.
(12) Yeni, Y. N.; Kim, D. G.; Dong, X. N.; Turner, A. S.; Les, C. M.; Fyhrie, D. P. *Clin. Orthop. Relat. Res.* **2006**, *443*, 101−8.
(13) Tai, K.; Ulm, F. J.; Ortiz, C. *Nano Lett.* **2006**, *6*, 2520−2525.
(14) Ingram, R. T.; Clarke, B. L.; Fisher, L. W.; Fitzpatrick, L. A. *J. Bone Miner. Res.* **1993**, *8*, 1019−1029.
(15) Giachelli, C. M.; Liaw, L.; Murry, C. E.; Schwartz, S. M.; Almeida, M. *Ann. NY Acad. Sci.* **1995**, *760*, 109−126.
(16) Liaw, L.; Skinner, M. P.; Raines, E. W.; Ross, R.; Cheresh, D. A.; Schwartz, S. M.; Giachelli, C. M. *J. Clin. Invest.* **1995**, *95*, 713−724.
(17) Kamat, S.; Su, X.; Ballarini, R.; Heuer, A. H. *Nature* **2000**, *405*, 1036−1040.
(18) Smith, B. L.; Schaffer, T. E.; Viani, M.; Thompson, J. B.; Frederick, N. A.; Kindt, J.; Belcher, A.; Stucky, G. D.; Morse, D. E.; Hansma, P. K. *Nature* **1999**, *399*, 761−763.
(19) Landis, W. J. *Bone* **1995**, *16*, 533−544.
(20) Aizenberg, J.; Weaver, J. C.; Thanawala, M. S.; Sundar, V. C.; Morse, D. E.; Fratzl, P. *Science* **2005**, *309*, 275−278.
(21) Fantner, G. E.; Birkedal, H.; Kindt, J. H.; Hassenkam, T.; Weaver, J. C.; Cutroni, J. A.; Bosma, B. L.; Bawazer, L.; Finch, M. M.; Cidade, G. A. G.; Morse, D. E.; Stucky, G. D.; Hansma, P. K. *Bone* **2004**, *35*, 1013−1022.
(22) Peterlik, H.; Roschger, P.; Klaushofer, K.; Fratzl, P. *Nat. Mater.* **2006**, *5*, 52−55.
(23) Thompson, J. B.; Kindt, J. H.; Drake, B.; Hansma, H. G.; Morse, D. E.; Hansma, P. K. *Nature* **2001**, *414*, 773−776.
(24) Fantner, G. E.; Oroudjev, E.; Schitter, G.; Golde, L. S.; Thurner, P.; Finch, M. M.; Turner, P.; Gutsmann, T.; Morse, D. E.; Hansma, H.; Hansma, P. K. *Biophys. J.* **2006**, *90*, 1411−1418.
(25) Thompson, J. B.; Hansma, H. G.; Hansma, P. K.; Plaxco, K. W. *J. Mol. Biol.* **2002**, *322*, 645−652.
(26) Rief, M.; Gautel, M.; Oesterhelt, F.; Fernandez, J. M.; Gaub, H. E. *Science* **1997**, *276*, 1109−1112.
(27) Rief, M.; Pascual, J.; Saraste, M.; Gaub, H. E. *J. Mol. Biol.* **1999**, *286*, 553−561.
(28) Fisher, L. W.; Torchia, D. A.; Fohr, B.; Young, M. F.; Fedarko, N. S. *Biochem. Biophys. Res. Commun.* **2001**, *280*, 460−465.
(29) Carrion-Vazquez, M.; Oberhauser, A. F.; Fowler, S. B.; Marszalek, P. E.; Broedel, S. E.; Clarke, J.; Fernandez, J. M. *Proc. Natl. Acad. Sci. U.S.A.* **1999**, *96*, 3694−3699.
(30) Oesterhelt, F.; Oesterhelt, D.; Pfeiffer, M.; Engel, A.; Gaub, H. E.; Muller, D. J. *Science* **2000**, *288*, 143−146.
(31) Bornschlogl, T.; Rief, M. *Phys. Rev. Lett.* **2006**, *96*, 118102.
(32) Labeit, S.; Kolmerer, B. *Science* **1995**, *270*, 293−296.
(33) Choquet, D.; Felsenfeld, D. P.; Sheetz, M. P. *Cell* **1997**, *88*, 39−48.
(34) Becker, N.; Oroudjev, E.; Mutz, S.; Cleveland, J. P.; Hansma, P. K.; Hayashi, C. Y.; Makarov, D. E.; Hansma, H. G. *Nat. Mater.* **2003**, *2*, 278−283.
(35) Oroudjev, E.; Soares, J.; Arcdiacono, S.; Thompson, J. B.; Fossey, S. A.; Hansma, H. G. *Proc. Natl. Acad. Sci. U.S.A.* **2002**, *99* , 9606.
(36) Boskey, A. L.; Maresca, M.; Ullrich, W.; Doty, S. B.; Butler, W. T.; Prince, C. W. *Bone Miner.* **1993**, *22*, 147−159.
(37) McKee, M. D.; Nanci, A. *Microsc. Res. Tech.* **1996**, *33*, 141−164.
(38) Chen, Y.; Bal, B. S.; Gorski, J. P. *J. Biol. Chem.* **1992**, *267*, 24871−24878.
(39) Gupta, H. S.; Wagermaier, W.; Zickler, G. A.; Hartmann, J.; Funari, S. S.; Roschger, P.; Wagner, H. D.; Fratzl, P. *Int. J. Fract.* **2006**, *139*, 425−436.
(40) Hansma, P. K.; Turner, P. J.; Ruoff, R. S. *Nanotechnology* **2007**, *18*, 044026.
(41) Thurner, P. J.; Erickson, B.; Jungmann, R.; Schriock, Z.; Weaver, J. C.; Fantner, G. E.; Schitter, G.; Morse, D. E.; Hansma, P. K. *Eng. Fract. Mech.* **2007**, *74*, 1928−1941.
(42) Kindt, J. H.; Thurner, P. J.; Lauer, M. E.; Bosma, B. L.; Schitter, G.; Fantner, G. E.; Izumi, M.; Weaver, J. C.; Morse, D. E.; Hansma, P. K. *Nanotechnology* **2007**, *18*, 135102.
(43) Christensen, B.; Nielsen, M. S.; Haselmann, K. F.; Petersen, T. E.; Sorensen, E. S. *Biochem. J.* **2005**, *390* (Pt 1), 285−292.
(44) Giachelli, C. M.; Schwartz, S. M.; Liaw, L. *Trends Cardiovasc. Med.* **1995**, *5*, 88−95.
(45) Qiu, S. R.; Wierzbicki, A.; Orme, C. A.; Cody, A. M.; Hoyer, J. R.; Nancollas, G. H.; Zepeda, S.; De Yoreo, J. J. *Proc. Natl. Acad. Sci. U.S.A.* **2004**, *101*, 1811−1815.
(46) Sheng, X.; Jung, T.; Wesson, J. A.; Ward, M. D. *Proc. Natl. Acad. Sci. U.S.A.* **2005**, *102*, 267−272.
(47) Nanci, A. *J. Struct. Biol.* **1999**, *126*, 256−269.
(48) Duvall, C. L.; Taylor, W. R.; Weiss, D.; Wojtowicz, A. M.; Guldberg, R. E. *J. Bone Miner. Res.* **2007**, *22*, 286−297.
(49) Seog, J.; Dean, D.; Plaas, A. H. K.; Wong-Palms, S.; Grodzinsky, A. J.; Ortiz, C. *Macromolecules* **2002**, *35*, 5601−5615.
(50) Robey, P. G., Bone matrix proteoglycans and glycoproteins. In *Principles of Bone Biology*; Bilezikian, J. P., Raisz, L. G., Rodan, G. A., Eds.; Academic Press: San Diego, 2002; Vol. 1, pp 225−237.
(51) Fedarko, N. S.; Fohr, B.; Robey, P. G.; Young, M. F.; Fisher, L. W. *J. Biol. Chem.* **2000**, *275*, 16666−16672.
(52) Blom, N.; Gammeltoft, S.; Brunak, S. *J. Mol. Biol.* **1999**, *294*, 1351−1362.

NL0712769